THE PENNSYLVANIA STATE UNIVERSITY
SCHREYER HONORS COLLEGE

DEPARTMENT OF CHEMICAL ENGINEERING

ULTRASENSITIVE BIOMOLECULAR DETECTION ENABLED BY NANOMATERIALS

VIKTOR A. ADALSTEINSSON

Spring 2010

A thesis
submitted in partial fulfillment
of the requirements
for a baccalaureate degree
in Chemical Engineering
with honors in Chemical Engineering

Reviewed and approved* by the following:

Jong-in Hahm
Assistant Professor of Chemical Engineering
Thesis Adviser

Themistoklis Matsoukas
Professor of Chemical Engineering
Honors Adviser

* Signatures are on file in the Schreyer Honors College

ABSTRACT

A review of various publications is first given as a background and introduction to the field of nanoscale biosensors. Afterwards, the actual biosensor development undertaken as honors thesis research is presented: the ultrasensitive detection of cytokines enabled by nanoscale ZnO arrays. By achieving subfemtogram per milliliter detection sensitivity in these ZnO nanoarray biosensors, cytokines implicated in the pathogenesis of acute kidney injury (AKI), such as interleukin-18 and tumor necrosis factor-α, may be identified at trace levels within human urine. In the clinical setting, this achievement holds great promise for permitting early disease detection and thereby, improving a patient's prognosis. A 3-4 order of magnitude increase in diagnostic power has been gained over conventional assays by exploiting the wide band gap and large exciton binding energy of nanoscale ZnO arrays in fluorescent assays. Measured signals are shown to directly correlate with cytokine concentrations in both direct and sandwich assays involving both pure buffer and urine. Therefore, robust, high-throughput biosensors with unparalleled levels of sensitivity have been developed and described for potential use in the early detection of cytokine-implicated diseases (Adalsteinsson et al. 2008).

TABLE OF CONTENTS

LIST OF FIGURES

ACKNOWLEDGEMENTS

I would like to thank Dr. Jong-in Hahm and Dr. Themistoklis Matsoukas for their guidance and support in pursuing undergraduate research. Given my expressed interests in laboratory work, Dr. Matsoukas suggested that I get involved with research as early as possible in my college career, so I explored various opportunities with professors in chemical engineering. Dr. Hahm was very responsive to letting me gain experience in her lab and was willing to serve as my thesis adviser starting when I was entering my second semester of freshman year. Her innovative thinking and expertise in merging nanotechnology and biological sciences fostered a great environment in which to complete my honors thesis.

Chapter 1

INTRODUCTION TO NANOSCALE BIOSENSORS

While nanomaterials have various applications from computer chips to medical devices to tissue engineering, the exploitation of these nanocrystalline materials shall be considered in the context of biosensor development. In particular, nanowires, nanoparticles, and thin films are presented for their desirable properties in biosensors, and this chapter communicates summary reviews of various publications in this area. Overall, the optical and magnetic properties of nanomaterials tend to have the greatest relevance to biological applications (Salata 2004). In the next chapter, an introduction to the actual thesis research, regarding the development of an ultrasensitive cytokine biosensor, is presented.

Since nanotechnology is such a new field, much of the relevant biosensor technology must be examined through previous studies involving nanomaterials applied in the detection schemes for various proteins and biomolecules. The subsequent publication reviews demonstrate the development concerns and assay schemes used in tandem with methods from cyclic voltammetry to surface plasmon resonance in order to achieve high detection sensitivity for biomolecules. By reviewing the experiments and techniques involved in the development of different biosensor platforms, an appreciation is gained for the considerations that needed to be addressed by the research groups. The nanomaterials chosen must be compatible with the biological system in order to prevent false positives and to promote a durable, reliable, and high-throughput sensor capable of either directly or indirectly detecting the analyte. In many cases, surface chemistry modifications are required for hybridizations of capture probe and analyte; meanwhile, it is desired to increase signal-to-noise ratio in order to distinguish sample from control. Yet, each platform calls for a unique development approach in order to best exploit the

functional properties of the nanomaterials in the most appropriate manner for the respective assay.

Surface Characterization of Indium-Tin Oxide Thin Electrode Films for Use as a Conducting Substrate in DNA Sensor Development (Moore et al. 2006)

ITO thin films have been a focus area of research for their desirable properties as a conductive substrate in biosensors, given their high optical transmittance in the near IR and visible frequencies and wide band gap. Modification of ITO thin films allows for numerous surface chemistry interactions, which may be used to immobilize molecules on biosensors. Meanwhile, it is critical to have the means to characterize surface structure and modifications of electrodes because those factors determine surface chemistry of the substrates. One technique for developing ITO thin films involves heat treatment annealing processes; however, this method leads to irregularities in grain size and shape as well as defects in the film. Therefore, a different method is commonly chosen to deposit ITO as a thin film using an e-beam evaporator and modified annealing conditions.

Silane chemistry modifications were chosen in this study as a surface connection between ITO thin film and 1,4-phenylene diisothiocyanate (PDITC) cross linkers. The PDITC was designed to immobilize DNA and therefore, has implications in biosensor technology. Since control of deposition and pretreatment parameters can have a major impact on the formation of alkylsilane self-assembled monolayers on ITO thin films, a reproducible fabrication process for modified thin films was also a crucial component of the development process. The films must be uniformly produced with desirable optical and conductivity properties; however, high optical transmittance in the visible frequencies typically indicates that the material has low conductivity

or high sheet resistance. Therefore, these properties need to be balanced in such a way that optical transmittance is relatively high while sheet resistance is maintained low.

In this study, epifluorescence images were captured with little loss in signal-to-noise ratio following immobilization of an oligonucleotide to the PDITC and subsequent hybridization with Cy3-labelled complimentary oligonucleotide. The average intensity of the line profiles in arbitrary units was compared when imaged from above and below the thin film with low background signals. As a result, the ITO thin film substrate presents a low signal-to-noise ratio platform that may be used with inverted microscopes, allowing for surface chemistry to also be developed between the substrate support and the ITO film. ITO is one of several metal oxide materials being explored in various biosensor platforms involving optical and electrical sensing.

Electrochemical Determination of Total Alkaline Phosphatase in Human Blood with a Micropatterned ITO Film (Kim & Juhyoun 2005)

Alkaline phosphatase is a highly stable, non-specific phosphomonoesterase enzyme, which facilitates the hydrolysis of phosphomonoesters in the human blood. The key product of the hydrolysis is usually inorganic phosphate. The enzyme, being derived from the liver and bone, has been tied to various conditions in the body. For instance, an increased level of alkaline phosphatase in the blood stream may signal a problem with the liver and bones, and the enzyme has been implicated as a disease marker for hepatitis, tumors, and cirrhosis. Although alkaline phosphatase is traditionally employed in ELISA assays where the product is monitored by spectroscopy or chemiluminescence, the products of enzyme catalysis have been also been evaluated by electrochemical methods. In doing so, the accuracy and speed of the assay may be increased. Effectively, the detection of alkaline phosphatase is conducted via an indirect mechanism in which the electroactive product of its catalysis is quantified.

In this study, indium tin oxide (ITO) had been chosen as the material for an alkaline phosphatase sensor due to many reasons. As a result of its low nucleophilicity, ITO does not favor the adsorption of organic molecules, but it can withstand metal deposition without binding strongly to metal adatoms. Furthermore, ITO, being in an oxidized state, can remain relatively un-reactive when under positive potential during voltammetry. Additionally, an electrochemical sensor of ITO film on glass can be developed rather easily using an office laser printer and transparency film to facilitate photolithography on the metal oxide film. In this sense, patterned electrodes and electrical connectors with micrometer spacing can be produced for use in electrochemical sensors.

In essence, a biosensor for alkaline phosphatase with *p*-nitrophenyl phosphate as a substrate was created using three electrodes (working, counter, and reference) on a single ITO film manipulated by simple, microscale photolithography. To develop a biosensor that functions in a solution of blood sera, it was necessary to consider the non-specific adsorption to the electrode of other organic molecules present in sera. Non-specific adsorption phenomena is a common concern when developing a biosensor, and experiments must be conducted to ensure that the measured signals from the assay do not have significant contributions from extraneous molecules. Chapter 4 explains how non-specific adsorption was evaluated in the actual research component of this thesis involving a novel ZnO nanoarray biosensor.

However, in this alkaline phosphatase biosensor development, gold, glassy carbon, and ITO were evaluated as electrode materials in an adsorption study. Both gold and glassy carbon electrodes exhibited electrochemical signals in pure fetal bovine serum, which suggested surface adsorption to those materials. On the other hand, ITO did not yield any significant electrochemical signal, which provided a level baseline up to a point at which the solution experiences electrolysis.

Alkaline phosphatase in both fetal bovine serum and human serum was analyzed using the ITO electrodes. The fetal bovine serum had been dialyzed, so it did not contain significant amounts of alkaline phosphatase. Voltammograms of fetal bovine serum, both with and without *p*-nitrophenyl phosphate, did not exhibit electrochemical signals up to the point of solution electrolysis. On the other hand, voltammetry of fetal bovine serum containing *p*-nitrophenyl phosphate and alkaline phosphatase yielded an electrochemical signal. Likewise, voltammetry of human serum using ITO electrodes did not yield a signal; yet, the solution of human serum and *p*-nitrophenyl phosphate produced an electrochemical signal, because human serum contains significant levels of alkaline phosphatase. In all cases of alkaline phosphatase detection, the signal was due to enzyme hydrolysis of *p*-nitrophenyl phosphate to *p*-nitrophenol, which can be detected electrochemically. Once again, this is an indirect means of detecting the enzyme.

Untreated blood samples were also tested with the ITO-based electrochemical sensor. Following addition of p-nitrophenyl phosphate to human blood and serum from the same person, square wave voltammetry was conducted using the ITO electrodes. Similar peaks were realized for the two samples from the same person; however, the whole blood exhibited a wider peak in the voltammogram. The results of such experiments were compared against the established method for determining alkaline phosphatase levels in blood: calorimetric detection of the hydrolyzed *p*-nitrophenol. The levels of alkaline phosphatase activity determined by the ITO-based electrochemical sensor matched closely the results of the calorimetric method, suggesting that the ITO platform in tandem with square wave voltammetry is effective in detecting alkaline phosphatase activity. Since the development of nanoscale biosensors is often based on improving current detection schemes, it is important to consider the efficacy of the novel sensor in comparison with conventional systems. For instance, the lower limit of detection of the ZnO nanoarray biosensors, developed as a result of this thesis research, are compared in Chapter 4 with the detection sensitivity of conventional ELISA assays for the same cytokines.

Optical Sensing of Electrochemical Reactions on a Bio-Hybrid Nanoparticle (Liu & Lee 2005)

Considering the major theme of nanoscale biosensors is to improve detection sensitivity over conventional assays, this objective was considered for assaying cytochrome c at low concentrations. In specific, a single Au nanoparticle plasmon was proposed as an electro-optical sensor, using scattering spectroscopy and dark-field microscopy to probe the plasmon resonance of single metallic nanoparticles. Since the optical range of elastic scattering for a metallic nanoparticle is larger than inelastic emissions including Raman scattering and fluorescence, a single Au nanoparticle has the potential to detect molecules with a high level of sensitivity. Single nanoparticle scattering spectroscopy can also be used to detect the binding of small molecules and proteins to the surface of Au nanoparticles.

Cytochrome c is a redox protein that serves a key role in electron transport for oxidation of substrates; yet, the lower level of detection for cytochrome c activity via cyclic voltammetry has potential to be improved. The change in conformation of cytochrome c from ferric to ferrous states can be measured optically with surface enhanced Raman spectroscopy or using surface plasmon resonance. Since the plasmon resonance wavelength of a nanoparticle will decrease as its free electron density is increased by factors such as ionic current flow, the use of single nanoparticle scattering spectroscopy in monitoring redox reactions on Au nanoparticles has been investigated. Additionally, conjugated complexes of cytochrome c and Au nanoparticles have been generated to study changes in plasmon resonance wavelength when the enzyme catalyzes a redox reaction and, thereby, generates an ionic current flow.

In this study, the simultaneous plasmon resonance scattering and electrochemical signal from cyclic voltammetry on Au-cytochrome c complexes linked to ITO on glass electrodes was evaluated. Ferrous cytochrome c was connected to an ITO electrode via a molecular bridge to uniform Au nanoparticles, which were connected to the ITO electrode. Essentially, the bridge

from enzyme to Au nanoparticle was caused by electrostatic contact between lysine groups in cytochrome c and the carboxyl group in 3-mercaptopropionic acid, which was used to modify the surface of the Au nanoparticles. Such a molecular bridge generated an effective electron transfer path with little barrier to electron tunneling. Quartz crystal microbalance measurements could even be used to estimate a maximum load density of cytochrome c on Au nanoparticles, and the docking of cytochrome c to Au nanoparticles was confirmed by dark-field microscopy before and after conjugation. A red shift of plasmon resonance peak occurred following addition of cytochrome c to the surface-modified Au nanoparticles, but the scattering spectrum of a single Au nanoparticle was monitored as the potential through the ITO electrode was swept. As the working potential approached the oxidation potential of the enzyme, electrons from the ferrous heme groups of cytochrome c molecules were sent through the Au nanoparticle to the ITO electrode. As a result, the free electron density in the nanoparticles increased, and the plasmon resonance wavelength continued to blue-shift until the oxidation potential was reached at the ITO electrode.

Moreover, the scattering intensity of the Au-cytochrome c complex decreases, because the radius of ferrous cytochrome c molecules is larger than ferric cytochrome c molecules. This is due to the fact that Rayleigh scattering intensity is directly related to radius raised to the sixth power. Consequently, the blue shift was thought to be party due to the change in radius of cytochrome c when undergoing conformational change from ferrous to ferric state. Yet, once the oxidation potential of cytochrome c is exceeded, the free electron density decreases in the Au nanoparticles because all of the heme groups have been oxidized. This causes red-shift in the plasmon resonance spectra, but blue-shift occurs again when the potential is subsequently reduced below the oxidation potential, as in cyclic voltammetry. As a result, a blue-shift peak can be noted when the reduction potential is reached by the working electrode. Consequently, this sensor scheme presents a novel system for hybrid opto-electronic detection of redox

enzymes. In this case, the plasmon resonance spectra had to be considered in tandem with working potential because of the effects of oxidation state on the radius of the enzyme and the free electron density in the nanoparticle.

Nanocatalyst-Based Assay Using DNA-Conjugated Au Nanoparticles for Electrochemical DNA Detection (Selvaraju et al. 2008)

As opposed to using nanoparticles to create a hybrid optical and electrical sensor by creating molecular bridges and docking sites for redox enzymes, nanoparticles may also be used as nanocatalysts. Consider the system presented by Kim & Juhyoun 2005 for alkaline phosphatase detection; had the objective been to detect *p*-nitrophenyl phosphate, the enzyme would have simply been the mediator to allow for *p*-nitrophenyl phosphate to be converted to electroactive product, which would be detectable by cyclic voltammetry. Given this realization, it is understandable why enzymes have valid applications in biosensor platforms; meanwhile, this research group attempts to replace enzyme-mediated systems with nanoparticles for the subsequent reasons. While enzymes are typically employed in bioassays and biosensors, their poor long-term stability and complicated preparation protocols create the need for more durable catalysts. Although enzymes have high specificity for target biomolecules, nanocatalysts have great potential to replace enzymes in some biosensors. Nanocatalysts have been employed in electrocatalysis and organic synthesis, and they tend to have many more active sites on their surface than enzymes. Furthermore, monodisperse nanocatalysts may be directly prepared with uniform size and exhibit high stability.

In order to achieve reproducible results in biosensor assays with nanocatalysts, deposition time and temperature must be optimized. While nanocatalysts have not been used as labels in many prior applications, they have the capability to provide decent signal generation and

amplification given the number of active sites that they have on their surface. Once again, the signal amplification effect is a very desirable property of nanomaterials for use in biosensor development. In particular, gold nanoparticles have been studied for use as labels in ultrasensitive protein detection.

After the conjugation of a nanocatalyst to a biomolecule, active sites on the nanocatalyst must remain accessible to substrate molecules; fortunately, previous studies revealed that many pinholes remained accessible on gold nanoparticles following adsorption of antibodies. In order to conjugate DNA to gold nanoparticles, thiolated self-assembled monolayers were employed to serve as physical barriers to allow for hybridization of nonspecifically bound single-stranded DNA. However, the accessibility of catalytic sites to negatively charged substrates on hybridized DNA-nanocatalyst surfaces may be limited due to the high negative charge of DNA. Such affinity considerations and charge interactions are crucial when trying to develop an effective biosensor.

While nanoparticles can be used as both catalytic and electrocatalytic labels, it is important to minimize the electrocatalytic reaction if it is not reproducible. Therefore, the magnetic beads are commonly used to reduce the electrocatalytic function of the nanoparticles by increasing the distance between gold nanocatalyst and electrode. Most electrochemical biosensors have electrodes that also act to immobilize analyte molecules. Yet, the beads merely serve as binding surfaces for target molecules, and they do not function as electrodes in magnetic bead-based sensors. Gold nanoparticle labels then bio-specifically attach to the magnetic beads, which become magnetically attracted to the electrode. Although, electron transfer between the gold nanoparticle and the electrode is limited when there is a low density of gold nanoparticles on the magnetic beads.

Effectively, a sandwich assay scheme was used with gold nanoparticles as catalytic labels in this study. The capture probes were biotinylated and immobilized to magnetic beads coated

with streptavidin. Following hybridization of DNA to capture-probe-conjugated magnetic beads, the detection probe, conjugated to the gold nanoparticles, was able to hybridize to the DNA. Then, the entire complex was attracted by a magnet to an ITO electrode that had been partially modified with ferrocene-modified dendrimers. Incubation of the resulting system with *p*-nitrophenol and $NaBH_4$ yielded electroactive *p*-aminophenol that could be electrooxidized to *p*-quinoneimine by ferrocene-mediated electron transfer. Effectively, redox cycling occurs for the interconversion of *p*-aminophenol and *p*-quinoneimine with $NaBH_4$ as a reducing agent and for electrooxidation processes. Moreover, bio-specific binding of DNA-conjugated gold nanoparticles occurs with magnetic beads, and the ITO electrode is the only signal-generating surface.

When the process was tested without magnetic beads, using the electrode to also immobilize the target, nonspecific binding was observed for probe-conjugated gold nanoparticles, and electrocatalytic oxidation of $NaBH_4$ by gold nanoparticles occurred. In other words, magnetic beads were necessary to maintain a high signal-to-noise ratio with this sensor platform. Furthermore, the peak current in cyclic voltammetry was higher for solutions containing higher concentrations of target DNA. The lower limit of detection for target DNA was found to be in the femtomolar range for this assay scheme, and nonspecific binding proved to be negligible to the performance of the sensor. Additionally, a linear detection range was noted from target DNA concentrations from 1 to 100 femtomolar; in this range, peak anodic current was linearly related to target DNA concentration. It was also found that hydridization of single-base-mismatched DNA was insignificant with the capture probe. Effectively, the sensor could distinguish between target DNA and single-base-mismatched or noncomplementary DNA.

Morphology-Dependent Electrochemistry of Cytochrome C at Au Colloid-Modified SnO_2 Electrodes (Brown et al. 1996)

In further consideration of cytochrome c detection, the morphology of the system must be evaluated. Electrochemical biosensors require an interface between a redox protein and an electrode that permits direct electron transfer without denaturation of the protein. Since conformational and functional changes may occur when the protein is contacted with uncoated metal, it is important to prevent that direct contact by modifying either the protein or electrode. Nanometer-sized, colloidal Au particles have been electrostatically bound to protein conjugates without affecting biological activity, and an electrochemical glucose biosensor has been created utilizing such Au nanoparticles. Additionally, uncoated, 12nm-diameter, colloidal Au particles have been used on SnO_2 in the reversible cyclic voltammetry of horse heart cytochrome c in solution. Yet, nanoscale morphology plays an important role in the reversibility and behavior of such proteins in cyclic voltammetry, because the colloidal Au nanoparticles serve as isolated microelectrodes.

The two pathways that have been previously shown to facilitate the electron transfer from redox metalloproteins include using mediators or promoters as electroactive or electroinactive intermediates, respectively, between electrodes and solution couples. However, colloidal Au nanoparticles do not fit either of these categories because electron transfer occurs at the interface of Au and solution. The particles essentially funnel electrons between electrode and electrolyte by allowing close approach of cytochrome c's heme cleft with positive dipole moment to the negatively charged colloidal Au surface. Additionally, the state of adsorption needs to be considered in terms of electrochemical impact. Irreversible cytochrome c adsorption has been associated with poor voltammetric results, and this sort of adsorption may be promoted by aggregated particles. For reversible cyclic voltammetry to be possible, the redox enzyme must be adsorbed in a reversible manner using isolated, colloidal particles, as opposed to aggregated

particles. While cytochrome c exhibits reversible voltammetry for isolated, colloidal Au particles, the morphology of such particles is crucial to the overall monitoring of the electrochemistry of redox enzymes. Therefore, derivatizing SnO_2 electrodes with colloidal Au particles of controlled morphology allows for reversible voltammetry of cytochrome c by preventing protein-metal contact and permitting reversible adsorption of the enzyme.

Cholesterol Biosensors Prepared by Layer-by-Layer Technique (Ram et al. 2001)

Amperometric biosensors require immobilization of an enzyme to the electrode surface. Various methods for this immobilization include simple adsorption, covalent binding, Langmuir-Blodgett, and layer-by-layer processes. Layer-by-layer techniques have been recently employed in biosensors and bioelectro-synthesis. Cholesterol oxidase is a redox enzyme that catalyzes the isomerization and oxidation of 3ß-hydroxysteroids. Cholesterol becomes oxidized to cholest-4-en-3-one, and the isomerization may be carried out without oxidation, as it binds steroid substrate following interaction with lipid bilayers.

Cholesterol oxidase and cholesterol esterase are typically used in conjunction to track native and esterified cholesterol levels. Since 70% of cholesterol is found in the esterified form in the body, it is important to observe both enzymes when determining total cholesterol levels in a patient. Most cholesterol tests involve spectrophotometric methods using an indirect enzyme assay following precipitation of lipoproteins. Since the enzyme must be used in each procedure, the conventional cholesterol test is rather costly. For amperometric cholesterol determination, an enzyme is also used, and there have been stability issues with enzymatic activity decreasing over time.

In this study, layer-by-layer deposition was controlled by adjusting pH above enzyme pI in order to make the protein solution negatively charged and adsorb to a positively charged layer.

Alternating depositions of polycations (PEI) and cholesterol oxidase were performed, and various analytical methods such as optical measurements, quartz crystal microbalance, and atomic force microscopy were used to monitor layer-by-layer deposition. Linearity was noted in a plot of UV-vis absorbance versus number of bilayers, indicating that PEI/cholesterol oxidase may be deposited using the layer-by-layer method. Also, quartz crystal microbalance analysis revealed linearity in frequency shifts versus deposition time for the layer-by-layer self-assembly of PEI/cholesterol oxidase on poly(styrene sulphonate)-coated quartz plates. Meanwhile, atomic force microscopy revealed the morphology of layer-by-layer depositions, and cholesterol oxidase molecules were observed to be granular with average grain height being 15.3 nm.

Cyclic voltammetry was first conducted on cholesterol oxidase in phosphate buffer, and the process was deemed reversible with a closed cycle. A similar approach was taken in the thesis research presented in Chapters 2-5: proof-of-concept experiments were first conducted involving analyte in pure buffer. Meanwhile, in this cholesterol oxidase study, cyclic voltammetry on ten bilayers of polycation and enzyme, on a platinum surface, also demonstrated reversibility. A closed cyclic voltammogram at different scan rates was observed for the surface confined enzyme, and the higher scan rate lacked a peak potential for oxidation. Additionally, linearity was noted for current density versus number of bilayers from electrochemical analysis at a fixed scan rate. In terms of biosensor stability, cyclic voltammetry was conducted on the 15-bilayer system after seven months. The cyclic voltammogram revealed a change in redox peak potential after that amount of time, and addition of cholesterol yielded also a changed peak potential with an increased cathodic peak. Consequently, it was suggested that the layer-by-layer deposited protein films may be active.

Characterization of Thin Poly(Pyrrole-Benzophenone) Film Morphologies Electropolymerized on Indium Tin Oxide Coated Optic Fibers for Electrochemical and Optical Biosensing (Konry et al. 2008)

The effectiveness of biosensors in the optical and electrochemical settings can be affected by varying electropolymerization parameters that control morphology and properties in the deposition of photoactive polymers for immobilization purposes. For instance, polypyrrole has been studied for potential use in biosensors and solid state devices due to its ability to be electrochemically deposited onto many different types of conducting anodes, including glassy carbon, graphite, and noble metals. Meanwhile, ITO has been used as an optically-transparent, conductive substrate to coat non-conductive fiber optics. ITO-coated fibers allow for the electrogeneration of poly(pyrrole-biotin) or poly(pyrrole-benzophenone) films using electrochemical deposition on surfaces that exhibit conductive as well as fiber optic properties. The biotin-functionalized polymer material can then be used to immobilize particular protein subunits via the biotin-avidin linkage. Yet, this immobilization method produces a monolayer between biotinylated polymer film and biotinylated protein, which may decrease effective transduction, indicating docking of antibodies to the protein.

To reduce transduction attenuation by an avidin monolayer, photoactive poly(pyrrole-benzophenone) can be used to directly immobilize protein on the polymer using UV illumination. Such a photo-electrochemical immobilization may be used with other biomolecules in biosensor applications. In this study, pyrrole-benzophenone was deposited onto ITO-modified optic fiber tips, and cholera toxin B was photo-immobilized onto the polymer coating. In generating the photo-active polymer monolayer, it was found that the formation of poly(pyrrole-benzophenone) becomes blocked by an insulating layer if potential oxidation is greater than the threshold for over-oxidation. Experiments were performed to evaluate electro-deposited film in immunosensor applications. Cholera toxin subunit B (CTB) was photoimmobilized to the substrate through a

reaction between the benzophenone group in the polymer and the carbon-hydrogen bonds in the protein. The chemiluminescent oxidation of luminol by hydrogen peroxide was catalyzed by the perixodase conjugated to a secondary antibody, which also served as a marker. Non-specific interactions were tested, and the response was seen to be only a small percentage of the normal response; therefore, the sensor demonstrated high specificity in immunosensor response.

In terms of optical sensing, the chemiluminescence response increased with polymerization time until thickening of polypyrrole film led to attenuated light collection. While the lower limit of detection for CTB analyte was 40ng/mL for the immunoassay, a different detection method was also tested. The electrochemical monitoring of redox activity of HRP that was bound to the secondary antibody from the immunoassay allowed for analyte concentration to be resolved down to 80ng/mL. Since ELISA methods boast a 100ng/mL lower limit of detection for CTB, the electrochemical and optical detection techniques proved to be rather effective. However, this platform did not demonstrate a significant increase in detection power over conventional ELISA assays.

An Interleukin-6 ZnO/SiO2/Si Surface Acoustic Wave Biosensor (Krishnamoorthy et al. 2008)

While microbiological assays are conventional techniques of detecting proteins, the sample collection and incubation required for such methods are complicated, and these procedures cannot always measure with high sensitivity. Surface acoustic wave (SAW) devices include mass transducers whose size may be reduced to develop micro-array platforms. While protein immunosensors have been developed using shear horizontal surface acoustic wave (SH-SAW) technology on quartz, they have low electromechanical coupling coefficients, low dielectric permittivity compared to the liquid media, and large penetration depth. Similar devices

on $LiTaO_3$ have issues with attenuation of acoustic waves due to the crystal's excitation of bulk acoustic waves. However, zinc oxide (ZnO) nanomaterials offer a large electromechanical coupling coefficient, the ability to bind biomaterials, and strong piezoelectric properties. ZnO/quartz immunosensors have reported decent results in previous studies. Yet, the incorporation of ZnO in epitaxial thin films on SiO_2/Si substrates allows for integration of CMOS technology and signal processing circuitry.

Interleukin-6 (IL-6) is a variably glycosylated glycoprotein whose production and secretion is associated with cell activation. Stress and age-related conditions such as osteoporosis, arthritis, cardiovascular disease, and certain cancers may lead to elevated levels of IL-6 in the blood stream. Normal levels of IL-6 in human blood range from 1 to 10 pg/mL. Being a critical indicator of particular health issues associated with age in patients, IL-6 is particular protein of interest to detect using biosensors.

In this study, anti-IL-6 was first adsorbed to the ZnO surfaces as a capture antibody, and pairs and clusters of antibody-protein binding were observed with SEM following deposition of IL-6. The immobilization of antibody on the gluteraldehyde-modified ZnO surface was driven by binding of the terminal aldehyde group of gluteraldehyde to the amine group of the antibody. The morphology of surface antibody immobilization was similar for gluteraldehyde binding versus direct adsorption to plain ZnO, and both loaded and unloaded resonant frequencies were taken for two different frequency sensors with and without immobilized protein, respectively. Taking the difference between those two frequency values allows for extrapolating the mass of protein immobilized on the sensor since the sensitivity of the device was known, and the higher frequency device provided greater frequency shifts with applied protein than the lower frequency device.

It was determined that direct surface antibody adsorption was not an effective attachment process for protein detection in this sensor platform. The measured IL-6 mass was always

significantly lower than the applied IL-6 mass, indicating that little protein was actually immobilized by the biosensor. Yet, the sensor was capable of measuring masses in the sub-femtogram range despite its poor adsorption ability. Furthermore, the amount of IL-6 adsorbed to the sensor window may be drastically increased through use of intermediary agents such as aminopropyltriethoxysilane (ATES) and gluteraldehyde. As a result, the measured IL-6 mass versus applied IL-6 mass exhibited a linear trend in this case for both sensors. However, a better linear fit was observed for the higher frequency sensor, and the low frequency sensor indicated some possible nonspecific adsorption by its slight deviations from linearity. A linear trend for mass measured versus mass applied was noted for immobilization of IL-6 through antibody for concentrations of IL-6 protein between 20 ng/mL and 2 μg/mL, and linearity for the higher frequency device was nearly perfect. Yet, since direct adsorption of protein played little role in the detection scheme, immobilization of protein would be necessary by monoclonal antibodies.

Zinc Oxide/Redox Mediator Composite Films-Based Sensor for Electrochemical Detection of Important Biomolecules (Tang et al. 2008)

The wide band gap and optical transparency of ZnO lend it to be an important nanomaterial in a variety of opto-electric applications. ZnO is also tolerable to the environment, has biocompatibility, and is rather inexpensive to purchase. Furthermore, hybrid polymer/inorganic materials have been used to enhance functionality of inorganic semiconductors, especially as nanocomposites.

Early disease detection efforts have led to the development of biosensors capable of identifying various levels of proteins associated with particular conditions. For instance, dopamine is a neurotransmitter in the catecholamine family, and the loss of neurons containing dopamine has been tied to diseases such as Parkinsonism. Yet, while dopamine may be easily

oxidized, allowing it to be detected by electrochemical means, many interfering compounds such as ascorbic acid and uric acid prevent its facile detection. Ascorbic acid is present at high levels in the central nervous system's extracellular fluid, and uric acid is the end product of metabolized purines. These compounds interfere with dopamine detection, because they exhibit nearly the same voltammetric response when oxidized at bare electrodes. However, uric acid levels are also important to quantify since abnormal levels have been associated with gout, uricemia, and Lesch-Nyan disease. Therefore, it becomes necessary to develop an electrochemical sensor capable of distinguishing voltammetric signals from dopamine, uric acid, and ascorbic acid. Systems have been reported for such applications using modified platinum, glassy carbon, and gold electrodes. Additionally, electrosynthesized polymers may be used to modify electrodes by forming polymeric films. For instance, the covalent modification of electrodes with poly(chromotrope 2B) and poly(vinyl alcohol) has been used in the simultaneous detection of ascorbic acid, uric acid, and dopamine. Various other electrode modifications have been reported for the simultaneous determination of uric acid, ascorbic acid, and dopamine levels. However, the electrochemical oxidation of serotonin forms a redox mediator that may be deposited atop a ZnO-coated glassy carbon electrode (GCE). This hybrid film coat is found to permit quantification of different component levels by distinguishing different electrochemical signals.

In this study, serotonin was electrochemically oxidized onto a GCE/ZnO-modified electrode under an irreversible process, and cyclic voltammetry confirmed the irreversible oxidation peak due to serotonin monomer oxidation. The voltammograms exhibited by sequential potential scans exhibited similar behavior as reported for polyazine, which suggested that a permanent rise in irreversible oxidation current for monomer describes the catalytic behavior and electronic conductivity of the resulting electrode. In other words, the increase in monomer oxidation during film growth may be indicative of a highly conductive polymer, and this also described the continuous adsorption of oxidation product onto electrode surface.

Therefore, redox mediators were electrodeposited onto ZnO-modified GCE surfaces, and the applied film appeared as a uniform, light blue coat, clearly visible on the electrode surface. The redox mediator formed was 5,5'-dihydroxy-4,4'-bitryptamine and contained a redox-active quinone-imine structure. While all oxidation products of serotonin have a high adsorption affinity for GCE, the redox mediators appeared to be most readily adsorbed.

Cyclic voltammetry was conducted on the GCE/ZnO/redox mediator-coated electrode in acidic solution, and two reversible redox peaks were noted for electrogenerated 4,5-dihydroxytryptamine (DHT) and tryptamine-4,5-dione (TAD). Anodic to cathodic peak current ratio was nearly equal to one, indicating a highly reversible process, and the peak currents depended linearly on scan rate. Furthermore, two redox peaks were noted at a low scan rate, and the separation in peak potentials should be zero for an ideal system. However, a nonzero peak potential separation has been noted for most modified electrode systems and may be due to slow electron transfer kinetics. An equation was developed to relate peak current as a function of surface coverage concentration, electrode surface area, and scan rate. Additionally, the formal potentials of reversible redox peaks shifted negatively with increased pH. Atomic force microscopy and scanning electron microscopy were used to characterize the film thickness and ZnO/redox mediator core/shell particles sizes and confirm the presence of redox mediators on the surface. AFM can be a very powerful technique in biosensor development, and Chapter 4 presents its use in evaluating adsorption to a Si substrate.

The electrocatalytic oxidation of dopamine from solution was carried out at the modified electrodes both with and without redox mediators. Better enhancement of redox peaks and a more reversible electrochemical process was noted for the electrodes with redox mediator modification. Moreover, at bare electrodes, ascorbic acid, uric acid, and dopamine have previously exhibited similar peak potentials for oxidation; whereas, cyclic voltammetry using the GCE/ZnO/redox mediator-modified electrode in a phosphate-buffered solution of ascorbic acid,

uric acid, and dopamine, yielded three separate oxidation peaks with decent peak-to-peak separations for the three aforementioned molecules.

The redox mediator DHT was found to efficiently mediate the oxidation of ascorbic acid as evidenced by a significant increase in anodic peak current with an oxidation potential for ascorbic acid being 60 mV less than the oxidation potential for DHT. Effectively, the anodic peak current was increased for all three components and may be due to hydrophobic and hydrophilic surfaces on the redox mediator film. Therefore, the electrochemical separation of ascorbic acid from dopamine may be explained by regions of the redox mediator film having different levels of hydrophobicity or hydrophilicity. Further experiments revealed that ZnO was not a critical component in the modified electrode design, but it helped promote electron transfer due to its high conductivity and large surface area for catalytic oxidation. Additionally, weak adsorption of ascorbic acid to ZnO was explained by the high pI, positively charged particles in neutral solution. Moreover, DHT and TAD redox systems performed better when ZnO was used in the modified electrode arrangement as a result of ZnO's semiconducting properties.

Although amperometric detection of dopamine is not practical when in the presence of ascorbic acid, reproducible signals were obtained for dopamine in the linear range from 6×10^{-6} to 1.2×10^{-4} M concentrations. Effectively, the GCE/ZnO/redox mediator-modified electrode exhibited higher electrocatalytic activity toward the oxidation of dopamine and was able to yield steady state signals within 5 seconds. The system was found to be precise and reliable in terms of measuring known concentrations of dopamine, ascorbic acid, and uric acid from real samples. However, the signals degraded to 85% of the original current response after 6 weeks, but the electrode current could remain stable after 600 cycles. Reproducibility and stability of an assay platform are clearly important considerations when evaluating for potential use in a clinical setting.

TiO_2 Phytate Films as Hosts and Conduits for Cytochrome C Electrochemistry (McKenzie et al. 2005)

Mesoporous oxides are commonly elected as components in biosensors to serve as electrocatalysts or modified electrodes. TiO_2 films, in particular, have been employed in different areas including photovoltaic, photocatalytic, and hydrophilic coating applications. The capability of metal oxides to immobilize biomolecules such as oligonucleotides, heme proteins, or redox enzymes has been a key area of research with regard to biosensor development, and metal oxides films are also desired for their ability to shuttle electrons.

Cytochrome c has been used at electrode surfaces in biosensors due to its redox function; in fact, it is sometimes considered the model system for electron transfer in biological systems. Cytochrome c has a positively charged outer shell containing much lysine and can mediate docking of the enzyme to a negatively charged surface. In particular, cytochrome c is readily adsorbed out of solution onto TiO_2 thin films of nanoparticles, assembled with phytic acid. The redox protein, being adsorbed to TiO_2 phytate films, may be indirectly immobilized onto ITO electrodes when the film is coated onto the electrode, and more redox enzyme may also be adsorbed as the thickness of the film is increased. Furthermore, TiO_2 phytate films will conduct electrons when in aqueous buffer, even though they are insulators in the dry state. These films may be coated onto non-conducting glass surfaces, and a porous gold layer may be further deposited to create a buried, modified electrode, known as a porotrode.

At modified ITO, gold, or platinum electrodes, the reduction of $Ru(NH_3)_6^{3+}$ in both aqueous and adsorbed states has exhibited voltammetric responses that vary with film thickness. In this study, reduction of $Ru(NH_3)_6^{3+}$ was carried out on both bare and modified ITO electrodes. While a reversible reduction response was realized for the process, a different voltammetric profile was observed for the TiO_2 phytate modified electrode. The difference in peak currents between oxidation and reduction stages was due to desorption of reduction product ($Ru(NH_3)_6^{2+}$)

into aqueous solution. Cyclic voltammetry was also conducted for the porotrode system in which a porous gold layer was sputter-coated atop a TiO_2 phytate modified non-conducting glass surface. In this setup, two redox peaks are noted: the peak at lower potential corresponds to the solution phase redox system, and the peak at higher potential is due to the immobilized redox system. The immobilized redox system's peak intensity in terms of current response scaled linearly with film thickness for up to 15 layers; furthermore, the porous gold coating enhanced the capacitance background current of the systems.

Effectively, TiO_2 phytate films are capable of immobilizing large quantities of cytochrome c in stable configurations for cyclic voltammetry, and well-defined redox peaks were noted for cytochrome c reduction at TiO_2 modified electrodes as well as at porotrodes. It was also determined that the peak current response in both of these systems was primarily due to immobilized enzyme, because it was orders of magnitude greater than the peak current predicted by the Randles-Sevcik expression for a diffusion-limited reduction process. Additionally, the reduction of cytochrome c can be achieved even after removing the electrode from solution, rinsing with water, and re-immersing in fresh electrode solution. Evidently, the cytochrome c was strongly immobilized on the TiO_2 phytate films. Results also suggested that diffusion limited processes dominate for film thicknesses greater than 300 nm and for high scan rates greater than 50 mV/s. Therefore, the process may be described by two regions on a scan rate versus membrane thickness plot: complete electrolysis and diffusion control. Additionally, for cytochrome c biosensor preparation, 3-mercaptopropionic acid was used to develop a stable bond between the membrane and gold surface while preventing the protein from blocking the electrode surface or becoming denaturized.

Most importantly, a linear relationship between peak current and amount of immobilized cytochrome c was realized with the sensor. Beyond a TiO_2 phytate film thickness of 20-30 layers and at a scan rate of 50 mV/s, the reduction response did not increase. Therefore, it became

necessary to understand the diffusion process within wet TiO_2 phytate films. The electron hopping process was expected to dominate diffusion effects at high concentrations of immobilized enzyme. Conductivity measurements were used to study the diffusion coefficient of electrons relative to the estimated diffusion coefficient for cytochrome c electron hopping through the TiO_2 membrane. As a result, it was postulated that cytochrome c is the rate-limiting step in the transport of electrons from the redox enzyme to the TiO_2 phytate film.

The conductivity of the probe dropped by an order of magnitude when cytochrome c was immobilized onto the TiO_2 phytate membrane. Evidently, TiO_2 served as the conduit for electron transport, but cytochrome c acted as a trapping state.

Tailoring Zinc Oxide Nanowires for High Performance Amperometric Glucose Sensor (Zang et al. 2007)

In terms of electron transport, amperometric glucose sensors require immobilization of the enzyme glucose oxidase and establishment of an electron tunnel between the enzyme and transducer. At the same time, the integrity of the enzyme must remain intact and the system must be mechanically stable. Nanostructured materials are commonly used to immobilize enzymes in biosensor applications, and certain metal nanoparticles and semiconductor nanomaterials have been shown to improve sensor performance. In particular, nanocrystalline metal oxides have high specific surface area and desirable properties for the adsorption of biomolecules. For instance, ZnO can immobilize proteins with high stability and little denaturation through electrostatic interactions due to its high isoelectric point.

In this study, the dimensionality of ZnO nanowires forming an enzyme electrode created a large surface area for enzyme adsorption. Yet, as will be shown in Chapter 4, ZnO nanoarrays were found to be rather poor at adsorbing enzyme relative to polymeric substrates; however, their

unique properties in terms of fluorescence-enhancement effects proved to drastically outweigh their protein adsorption characteristics. Nonetheless, to examine this present system with FESEM without losing glucose oxidase in the process, a membrane was formed atop the glucose oxidase bound to the nanowires by applying Nafion. Cyclic voltammetry was conducted on the Nafion/glucose oxidase/ZnO system both in the presence and absence of glucose. Reproducible voltammograms were noted, and anodic and cathodic peak potentials were clearly defined. The process was deemed to be between reversible and quasireversible due to relative anodic and cathodic peak potentials. However, cyclic voltammetry of ZnO in batteries is not reversible, suggesting that nanostructured ZnO has unique properties that enable at least quasireversible electrochemical redox reactions.

Chapter 2

RESEARCH MOTIVATION

The desire to detect cytokines at low concentrations is motivated by the prospect of detecting diseases at early stages and thereby, improving prognosis. Various cytokines have known implications in diseases, but it is necessary to develop an assay whose linear response range is capable of detecting elevated levels of such disease markers. Cytokines are effectively signaling peptides used by inflammatory and immune cells and have a large impact on inflammation, immune response, hemopoiesis, healing, and responses to injury (Whicher & Evans 1990).

The two cytokines chosen for study were interleukin-18 (IL18) and tumor necrosis factor-α (TNFα) given their implications in the pathogenesis of acute kidney injury (AKI). AKI is a serious condition with a 50% mortality rate, and it occurs in nearly 5-7% of hospitalized patients. As a result, it would be very beneficial to detect the onslaught of such illness at early stage before it becomes a life-threatening situation (Adalsteinsson et al. 2008).

The research was approached from a two-prong stance: proof-of-concept experiments were conducted first involving cytokines spiked in pure buffer and then involving cytokine spiked in urine. Conventional assay techniques present major limitations in terms of resolving low concentrations of cytokines, so it is critical to develop an assay capable of quantifying trace cytokine levels. Biomolecular detection based on fluorescent assays may be used in various settings from clinics to proteomics laboratories, but it requires a platform with high sensitivity and signal-to-noise ratio. Therefore, control experiments were required to ensure specificity of the assay as well as contributing factors to the fluorescence signal.

The following chapters have been adapted from our publication in the Journal of Analytical Chemistry, and the figures, figure captions, materials and methods, and appendix are drawn specifically from our published work (Adalsteinsson et al. 2008).

Chapter 3

MATERIALS AND METHODS

Preparation of Stripe- and Square- Array ZnO NR Platforms and Polymeric Substrates

Stripe- and square-arrays of ZnO NR platforms were fabricated using a gas-phase growth method as described in an earlier report. Si wafers (resistivity < 1 Ωcm, thickness: 0.017 inch) were obtained from Silicon Quest International (Santa Clara, CA). In order to achieve ZnO NR platforms directly upon the material's synthesis, 40nm Ag colloidal catalysts (Ted Pella Inc. Redding, CA) were first transferred to predetermined locations on Si wafers. The catalyst delivery was carried out by microcontact printing catalyst nanoparticles from a polydimethylsiloxane (PDMS) stamp that contained periodic patterns of 5 or 10 μm in width. ZnO NRs were then synthesized in a home-built chemical vapor deposition reactor at 950 °C for 1h under a constant flow of 100 standard cubic centimeters per minute of Ar. For various polymeric platforms, asymmetric PS-b-PVP diblock copolymer with an average molecular weight of 68,500 Da was obtained from Polymer Source Inc. (Montreal, Canada). PS with a molecular weight of 152,000 Da and PMMA with a molecular weight of 120,000 Da were obtained from Alfa Aesar (Ward Hill, MA). The diblock contained 70% of PS by weight with a polydispersity of 1.14. Si substrates were first cleaned with ethanol, acetone, and toluene and spun dry. Ultrathin films of PS-b-PVP, PS, and PMMA were spun cast from 0.5% (w/v) PS-b-PVP, 2% (w/v) PS, or 2% (w/v) PMMA in toluene, respectively, at 3500 rpm for 1 min onto Si substrates.

Preparation of Various Proteins and Antibodies

Bovine serum albumin (BSA) and horse radish peroxidase (HRP) were purchased from VWR Scientific Inc (West Chester, PA). The lyophilized powder of these protein molecules was reconstituted in PBS (10 mM mixture of Na_2HPO_4 and NaH_2PO_4, 140 mM NaCl, 3 mM KCl, pH 7.4) buffer or in deionized water, as recommended by the manufacturer. The reconstituted protein solutions were further diluted to various concentrations, as needed. 3, 3', 5, 5'-tetramethylbenzidine (TMB) solution containing 1.25 mM TMB and 2.21 mM H_2O_2 was obtained from VWR Scientific Inc (West Chester, PA). Recombinant IL-18 (Biovision, Mountain View, CA) and TNFα (MBL, Woburn, MA) were reconstituted in deionized water and stored in small aliquots at -80°C until use. The recombinant cytokines were added in varying concentrations to PBS or urine obtained from a healthy individual for use in calibrating the assay. A monoclonal anti human IL-18 antibody (clone 125-2H, MBL) was labeled with Alexa 488 using the Microscale Protein Labeling kit (Invitrogen Molecular Probes, Eugene, OR). Briefly, 50 μg of antibody (1 mg/ml) was mixed with 5 μl 1M $NaHCO_3$. Alexa 488 tetrafluorophenyl ester was added at a molar ratio of 70 and the mixture reacted for 30 minutes in the dark at room temperature. Labeled antibody was separated from free dye by centrifugation through a gel filtration column according to the manufacturer's instructions. The protein concentration and degree of labeling (DOL) were determined spectrophotometrically at 280 and 494 nm wavelengths. Generally, the antibody yield was 60-80% with a DOL of 5-11 molecules of dye/molecule of antibody. This antibody was used as the detection antibody for both the direct and sandwich IL-18 assays. A second, unlabeled IL-18 antibody (clone 159-12B, MBL) was used as the capture antibody in the sandwich IL-18 assay. A polyclonal rabbit anti-TNFα antibody (MBL) was used as the capture antibody for direct and sandwich TNFα assays. A

phycoerythrin-labeled (PE-labeled) rat anti-TNFα antibody (BD Biosciences, San Jose, CA) was used as the detection antibody for the TNFα immunoassay.

Direct Cytokine Assays

20µl aliquots of PBS buffer or urine containing various amounts of IL-18 or TNFα were deposited onto a NR platform and incubated for 15 min in a humidity-controlled environment at room temperature. After the incubation step, the platform was rinsed with PBS buffer multiple times. In order to passivate surface areas where no IL-18 or TNFα was bound, 20µl of 5 % BSA (w/v in PBS) was deposited onto the substrates. After 15 min of BSA blocking, the platform was rinsed with an ample amount of PBS buffer. Subsequently, 10µl of 2 µg/ml Alexa 488-labeled IL-18 antibody or 3 µg/ml PE-labeled TNFα antibody was placed onto the substrate and incubated for 30 min to allow the antibodies to bind to their respective target proteins. Following the incubation period, the sample was once again rinsed with PBS buffer multiple times. Immediately before fluorescence measurements, the sample was gently dried under a stream of N_2 gas.

Sandwich Cytokine Assays

20µl of 2µg/ml unlabeled IL-18 or TNFα antibody was deposited onto a ZnO NR platform. Following a 15 min incubation period in a humidity controlled chamber at room temperature, the platform was rinsed thoroughly with PBS buffer. 20µl of 5 % BSA (w/v in PBS) was then deposited onto the platform to block any remaining binding sites. After a 15 min of BSA blocking period, the sample was rinsed with an ample amount of PBS buffer. Then, 20µl aliquots of either PBS or human urine containing known amounts of IL-18 or TNFα were

deposited onto the platforms.. After a 15 min of further incubation, the platform was rinsed with PBS buffer. Subsequently, 10µl of 2µg/ml Alexa 488-labeled IL-18 antibody or 3µg/ml PE-labeled TNFα antibody was deposited to the above platform and incubated for 30 min. After the incubation period, the platform was rinsed with PBS buffer multiple times and gently dried under a stream of N_2 gas just before fluorescence imaging.

Enzyme-Linked Immunosorbent Assays (ELISA)

For comparison with the ZnO NR assays, levels of IL-18 and TNFα were measured using commercially available ELISA kits (IL-18 ELISA kit, MBL, Nagoya, Japan and Quantikine TNFα kit, R and D Systems, Minneapolis, MN) according to the manufacturers' protocols. Absorbance results, after subtraction of background, were normalized relative to the absorbance obtained using a standard containing 1000 picogram/ml cytokine.

Sample Characterization and Data Analysis

The size and shape of as-grown ZnO nanomaterials in the array platforms were characterized by using a scanning electron microscope, a FEI/Philips XL 20 operated at 20 kV. UV-vis absorbance spectra were subsequently recorded on a Hewlett Packard 8452A Diode Array Spectrophotometer. Fluorescence from the direct and sandwich assay samples was captured using a Zeiss Axio Imager A1m (Carl Zeiss Inc., Thornwood, NY). Fluorescence images were recorded with a Zeiss Axio CAM MRM digital camera and Axio-Vision software. Green fluorescence emission from IL-18 assays was characterized by excitation at 460-500 nm and collection at 510-560 nm. Red fluorescence emission from TNFα assays was obtained by excitation at 528-560 nm and collection at 570-645 nm. A computer software, Image Pro Plus

(Media Cybernetics Inc., Bethesda, MD), was used for subsequent image analysis. All concentration-dependent plots presented in this paper display data after subtracting the background signal that is measured by using assay solutions with no cytokine. The lowest detection limit is defined as the cytokine concentration for which the observed fluorescence signal exceeds the standard deviation of zero concentration data by a factor of 3.

Chapter 4

RESULTS AND DISCUSSION

ZnO Nanoarrays and Assay Design

Both sandwich and direct assays were conducted using samples of cytokine spiked in pure buffer and urine, and the ZnO nanoarray platforms were fabricated as described in Chapter 3. These dense-grown ZnO nanorods, arranged in periodic arrays on Si substrates, were used as the platform for the assays. Figure **4-1** shows SEM images of the actual nanorods in the biosensor platform. Evidently, uniform length, diameter, and crystalline structure are realized, and this consistency is important when developing a biosensor: the assay must be reliable and repeatable in order for it to have any useful application.

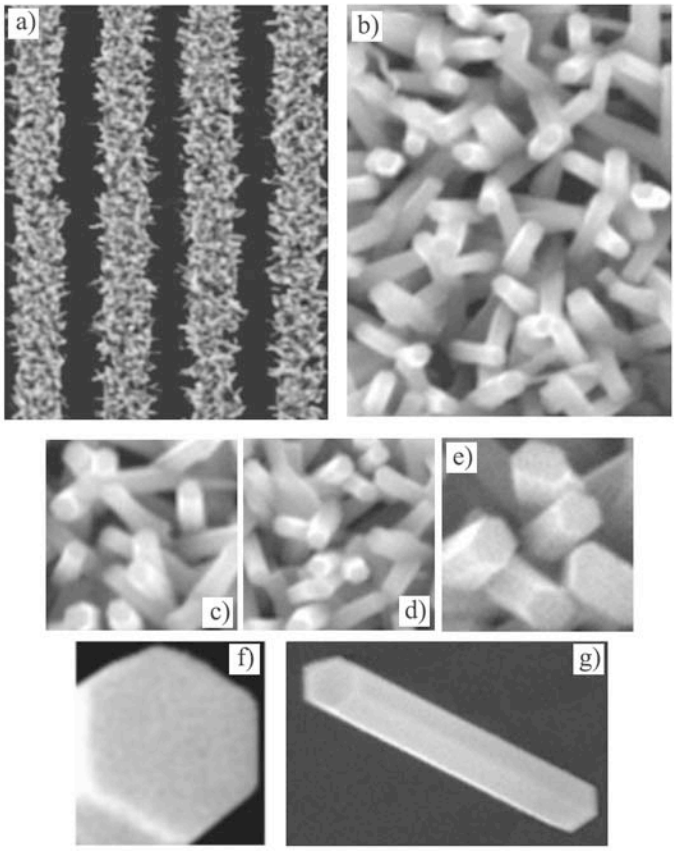

Figure **4-1**: SEM images of the stripe-array ZnO nanorod substrates. A uniform size and shape is exhibited by each array atop the Si substrate. The average diameter and length of the ZnO NRs are 180 nm and 1.2 μm, respectively. Individual ZnO NRs exhibit Wurtzite structures of high crystallinity and their preferential growths along the c-axis expose hexagonal end and side facets. Images (F) and (G) display high magnification images of (F) an end facet and (G) side facets. The SEM images correspond to scan areas of (A) 70 x 90 μm, (B) 3.5 x 4.5 μm, (C) 2 x 2 μm, (D) 2 x 2 μm, (E) 800 x 800 nm, (F) 200 x 200 nm, and (G) 763 x 1200 nm.

The average diameter and length of the nanorods varied by 12nm and 0.3μm, respectively, which constitute 6.7% and 25% variability in these dimensions. Meanwhile, Figure **4-2** exhibits the assay schemes employed in these experiments.

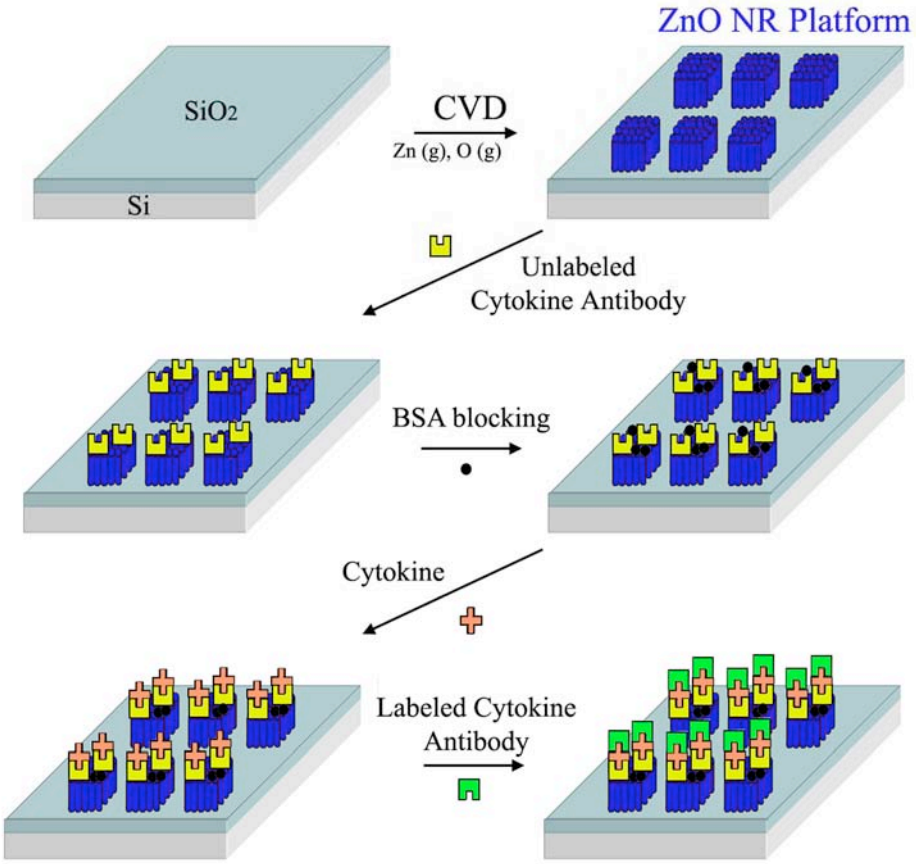

Figure **4-2**: Schematic illustration showing the overall assay scheme for the detection of cytokines. The illustration displays a sandwich assay scheme on a square ZnO NR platform that is assembled directly upon the NR synthesis in a chemical vapor deposition (CVD) reactor. Prefabricated square or stripe arrays of ZnO NRs are employed as fluorescence-enhancing detection platforms in the cytokine assays. For direct assays, cytokines in the sample are adsorbed onto ZnO NRs and then analyzed after incubating with their primary antibodies labeled with a fluorophore. For sandwich assays, primary antibodies pre-adsorbed onto ZnO NRs are incubated with samples containing cytokines. Then, secondary antibodies labeled with a fluorophore are further allowed to interact with the cytokines. Blocking steps are used both in direct and sandwich assays, unless indicated otherwise.

Proof-of-Concept: Fluorescence Enhancement Effects of ZnO Nanoarrays

In order to evaluate the fluorescence-enhancement effects of these ZnO nanoarray substrates, identical cytokine assays were carried out on both the nanoarrays as well as polymeric

substrates. The polymers that were spin-coated onto Si wafers for these experiments are common materials used in conventional microplates for other assays. Effectively, sandwich assays involving TNF-α were conducted on Si substrates spin coated with PS, PS-b-PVP, and PMMA, in addition to the ZnO nanoarrays. Capture antibodies were first deposited and noncovalently adsorbed to the substrates followed by blocking with BSA. Then, samples of pure buffer spiked with known amounts of TNF-α were incubated on the substrates, allowing for cytokine to be captured by the adsorbed, unlabelled anti-TNF-α antibodies. BSA was again used as a blocking agent to prevent non-specific capture of TNF-α. Finally, PE-labelled anti-TNF-α was incubated on the substrates in order to label the bound TNF-α with a PE tag. Subsequent fluorescent microscopy and image capture allowed for the fluorescence signals from each substrate to be quantified and normalized relative to the intensity obtained using 1 μg/ml of TNF-α on ZnO nanoarrays. The results of these experiments are shown in Figure **4-3a**.

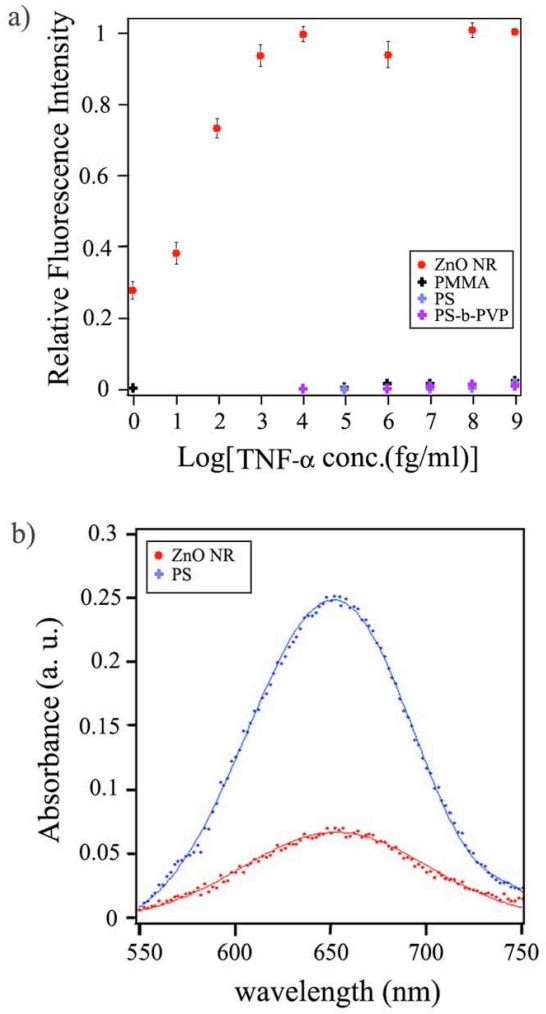

Figure **4-3**: (A) Comparison of fluorescence intensity obtained from various detection platforms after sandwich assays involving TNFα. After carrying out identical assays on ZnO NR, PS, PMMA, and PS-b-PVP platforms, the measured fluorescence signals at various TNFα concentrations were normalized with respect to the fluorescence intensity detected using 1 μg/ml of TNFα. The normalized fluorescence intensity was then plotted against the logarithmic value of the cytokine concentration. (B) UV-vis spectra comparing the amount of proteins on ZnO NR versus on PS platforms. Both platforms were treated identically with 50 μg/ml HRP and the characteristic absorbance peak of oxidized TMB product at 650 nm was subsequently recorded after 15 min of HRP-TMB assay.

The relative fluorescence intensity from assays conducted on ZnO nanoarray substrates was substantially higher than from the assays run on polymeric substrates. In fact, the ZnO nanoarrays permitted a fluorescence signal to be resolved for assays involving sub-femtogram per milliliter concentrations of TNF-α. Meanwhile, only weak fluorescence was exhibited by the

polymeric substrates across the range of concentrations tested. In order to verify that the apparent increase in fluorescence signal from the ZnO nanoarrays as compared to the polymeric substrates was not due to differences in adsorption phenomena, adsorption behavior was studied on both platforms. Since the nanorods are grown out of the plane of the Si wafer, it was postulated that this increased surface area relative to that of the flat polymer substrate may allow for a greater amount of capture antibody to be immobilized. Therefore, when the assay is finished, a larger amount of PE would be present in the system, leading to a more intense fluorescence signal.

In order to test this, HRP was nonspecifically adsorbed to both ZnO nanoarray and PS platforms of identical size under the same conditions. Then, TMB was used as a calorimetric reaction substrate to evaluate the amount of bound HRP by means of spectrophotometry. Figure **4-3b** shows the absorbance spectra from each platform, and it becomes evident that a much larger amount of HRP was adsorbed to the polymeric substrate. As a result, the enhanced fluorescence observed in the sandwich assays with TNF-α must not be due to increased nonspecific adsorption of capture antibody. Atomic force microscopy (AFM) also confirmed adsorption of biomolecules onto the exposed Si surface between arrays of nanorods on the ZnO nanoarray substrates. However, assays conducted on these platforms yielded no detectable fluorescence signal from these areas of the substrates. Consequently, the complex of unlabelled anti-TNF-α, TNF-α, and PE-labelled anti-TNF-α, produces a detectable fluorescence signal only when atop ZnO nanoarrays, for the low concentrations of TNF-α tested.

Assays Involving Cytokines in Pure Buffer

IL-18 and TNF-α, spiked at known concentrations within PBS buffer, were evaluated in direct and sandwich assays on the ZnO nanoarray substrates, and the results of these experiments are shown in Figure **4-4**.

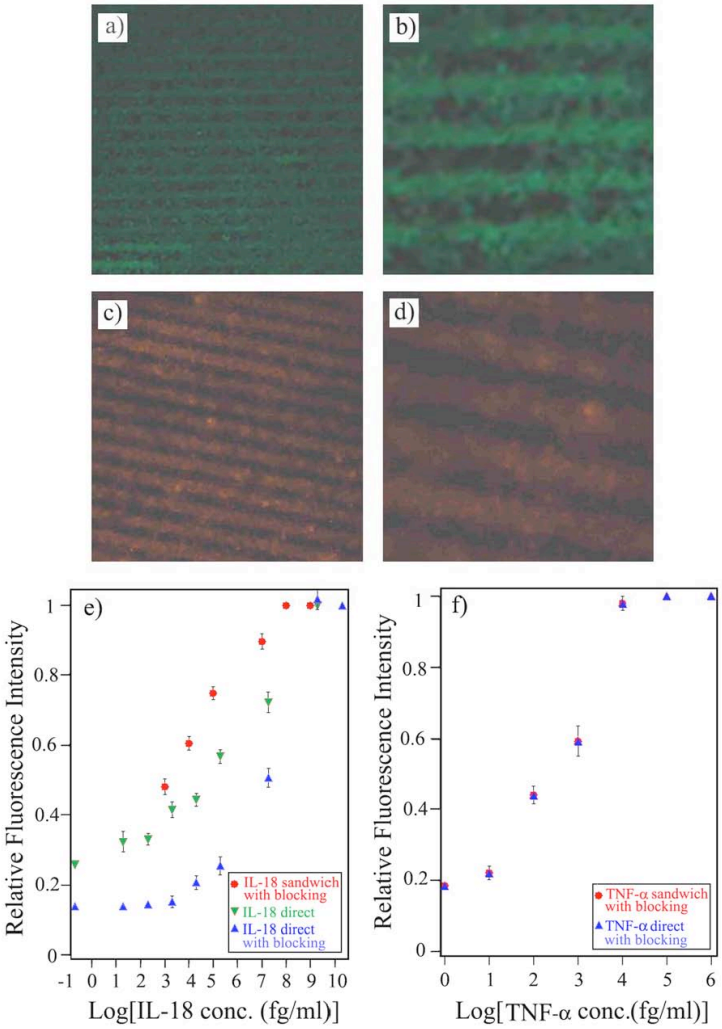

Figure **4-4**: Cytokine Assays in PBS buffer: Fluorescence images of 10 μm-period, stripe-array ZnO NR platforms after carrying out sandwich assays of cytokines diluted in PBS buffer. Panels of (A) 320 x 320 μm and (B) 100 x 100 μm display fluorescence images obtained from a sandwich assay involving 1 pg/ml of IL-18. Panels of (C) 250 x 250 μm and (D) 100 x 100 μm display fluorescence images obtained from a sandwich assay involving 1 pg/ml of TNFα. Brightness and contrast are adjusted in order to show the fluorescence images more clearly. (E and F) After performing various assays on stripe-array ZnO NR platforms, the measured fluorescence signals at various IL-18 concentrations were normalized with respect to the fluorescence intensity detected using 20 μg/ml of IL-18. The measured fluorescence signals at various TNFα concentrations were normalized with respect to the fluorescence intensity detected using 1 ng/ml of TNFα. The normalized fluorescence intensity is plotted against the logarithmic value of the cytokine concentration. Although not shown in the data set of TNFα, data points from direct assays without BSA blocking overlap with the data points from other TNFα assays shown in (F).

Within Figure 4-4, panels a and b show fluorescent images from assays involving 1 pg/mL of IL-18 in PBS buffer, and panels c and d show similar images from assays with 1 pg/mL of TNF-α in PBS buffer. Meanwhile, panels e and f exhibit the response range of the assay for IL-18 and TNF-α, respectively. As controls, ZnO nanoarrays without antibodies or cytokines proved to yield no fluorescence signal, and the fluorescence signal obtained from the assays on ZnO nanorods were clearly detectable over the background signal from exposed Si surface between arrays of nanorods. Furthermore, different fluorophores were found to produce varying fluorescence intensities. For instance, the Alexa 488 used for IL-18 assays produced higher fluorescence overall than the PE used for TNF-α assays. Evidently, there is potential to further improve the detection limit of these assays on ZnO nanoarray substrates by using alternative fluorophores.

For assay modes including sandwich, direct, and direct without blocking, femtogram per milliliter detection limits were approached. Assays yielded linear response ranges from 0.1 pg/mL to 10 ng/mL for IL-18 and from 0.01 pg/mL to 0.1ng/mL for TNF-α. Also, IL-18 direct assays without BSA blocking led to stronger fluorescence signals than the direct assays with blocking; meanwhile, sandwich assays exhibited higher signals than both of the direct IL-18 assays, with and without blocking. Potential explanations for this include enhanced binding of the capture antibody to the ZnO nanorods or greater accessibility of cytokine to the labeled anti-IL-18 detection antibody. Furthermore, steric effects with the ZnO nanorods have less impact on the sandwich assay given that the cytokine binds to the capture antibody, which has been immobilized to the nanorods, and the secondary detection antibody then binds the cytokine. Perhaps the detection antibody can then access the cytokine more effectively without as much steric hindrance. Nonetheless, little difference was noted between standard curves for TNF-α in sandwich and direct assay configurations.

Assays Involving Cytokines in Urine

Since sandwich assays produced great results with cytokine in pure buffer and to ensure the bio-specificity of the sensor when dealing with a complex media such as urine, each cytokine spiked in urine was examined via sandwich assays on ZnO nanoarray substrates. IL-18 and TNF-α were each formulated at known concentrations in urine, and the captured fluorescence from these assays is shown in Figures **4-5** and **4-6**.

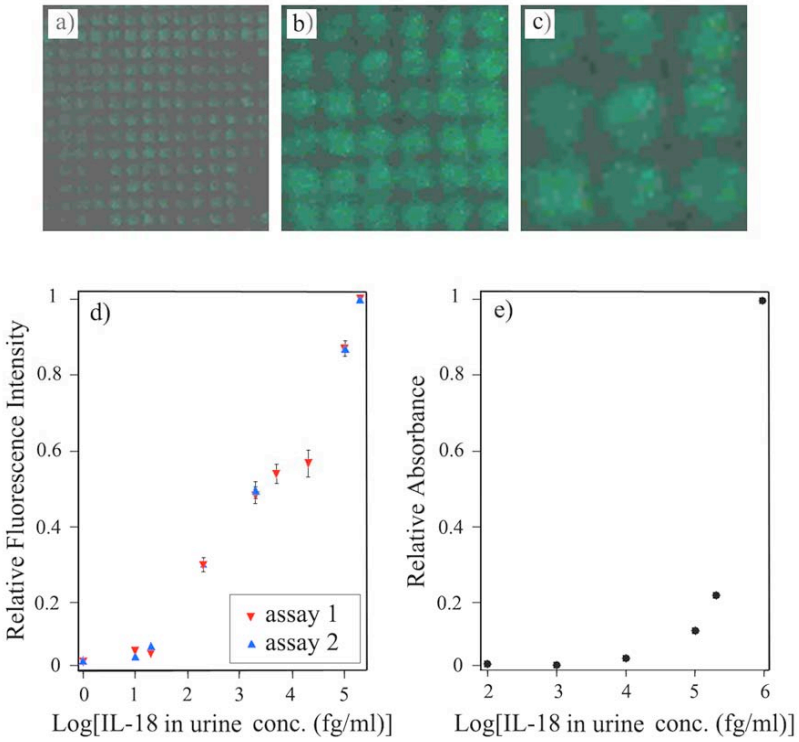

Figure **4-5**: IL-18 Assays in Urine: Fluorescence obtained from 5 μm-period, square-array ZnO NR platforms after carrying out IL-18 assays in urine. Panels (A) 140 x 140 μm, (B) 60 x 60 μm, and (C) 30 x 30 μm display fluorescence images obtained from a sandwich assay involving 20 fg/ml of IL-18 in urine. Brightness and contrast are adjusted in order to show the images more clearly. (D) After performing various assays on ZnO NR platforms, the measured fluorescence signals at various IL-18 concentrations in urine were normalized with respect to the fluorescence intensity detected when using 0.2 ng/ml of IL-18. The normalized fluorescence intensity is plotted against the logarithmic value of the IL-18 concentration. Assay results from two independent runs on ZnO NR platforms are displayed. (E) ELISA assay of urine containing the indicated amounts of IL-18. The measured absorbance signals at various IL-18 concentrations were normalized with respect to the absorbance detected using 1 ng/ml IL-18.

Within Figure **4-5**, panels a – c are fluorescence images captured from sandwich assays involving 20 fg/mL of IL-18 in urine. Likewise, panels a and b of Figure **4-6** depict fluorescence images from sandwich assays with 10 fg/mL of TNF-α. In both cases, the bright regions represent fluorescent signals from regions of ZnO nanorod population, and the dark areas are exposed Si surface between the actual nanorod arrays. Meanwhile, these figures also present a comparison of results from sandwich assays on ZnO nanoarray substrates versus the results from conventional ELISA assays, respectively. Evidently, the lower limit of detection of the ELISA method is approximately 10 pg/mL; whereas, the detection sensitivity of the sandwich assay on ZnO nanoarray substrates was around 1-10 fg/mL. Effectively, a 3-4 order of magnitude increase in detection power was gained over conventional ELISA assays for these cytokines in urine by using ZnO nanoarray platforms. Although urine contains a complex mixture of components, the assays conducted on ZnO nanoarray substrates proved to be very specific and sensitive with respect to each cytokine.

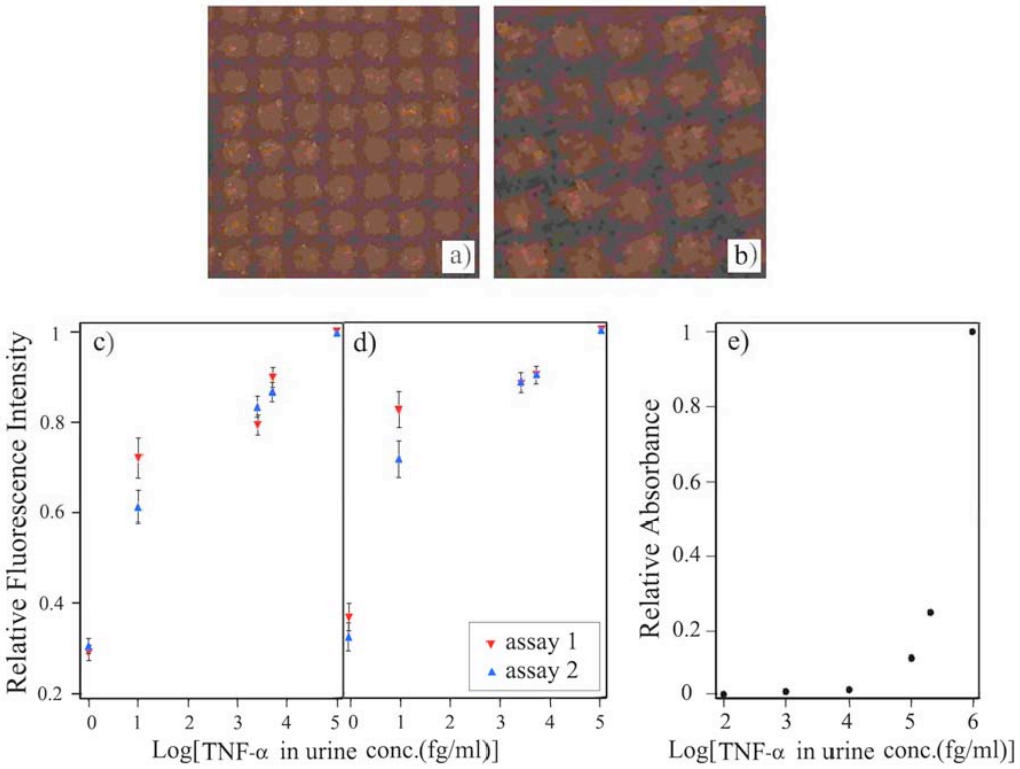

Figure **4-6**: TNFα Assays in Urine: Fluorescence obtained from 5 μm-period, square-array ZnO NR platforms after carrying out TNFα assays in urine. Panels (A) 90 x 90 μm and (B) 45 x 45 μm show fluorescence images obtained from a sandwich assay involving 10 fg/ml of TNFα in urine. Brightness and contrast are adjusted in order to show the fluorescence images more clearly. (C and D) After performing direct (C) and sandwich (D) assays on ZnO NR platforms, the measured fluorescence signals at various TNFα concentrations in urine were normalized with respect to the fluorescence intensity detected when using 0.1 ng/ml of TNFα. The normalized fluorescence intensity is plotted against the logarithmic value of the TNFα concentration. Assay results from two independent runs on ZnO NR platforms are displayed. (E) ELISA assay of urine containing the indicated amounts of TNFα. The measured absorbance signals at various TNFα concentrations were normalized with respect to the absorbance detected using 1 ng/ml TNFα.

Chapter 5

SUMMARY AND CONCLUSIONS

An ultrasensitive biosensor platform has been presented for the detection of cytokines IL-18 and TNF-α by exploiting the fluorescence signal-enhancing effects of nanoscale ZnO arrays. First, the assay schemes and ZnO nanoarray substrates were developed and described, and then proof-of-concept experiments were presented to demonstrate the unique properties of ZnO nanorods with respect to enhancing fluorescence signals. By comparing the protein adsorption characteristics of ZnO nanoarrays relative to polymeric substrates, it became evident that ZnO nanorods promote a substantially large enhancement of fluorescence signal intensity, despite immobilizing less protein. Furthermore, experiments with cytokine spiked in both pure buffer and urine revealed the power of the assay schemes with regarding to lower limit of detection and linear response range. Effectively, a 3-4 order of magnitude increase in detection power with respect to lower limit of detection was achieved over conventional techniques such as ELISA. As a result, the herein presented technology has been shown to improve fluorometric sensitivity in direct and sandwich cytokine assays. Furthermore, this novel platform holds great promise for clinical application by allowing for disease markers to be detected at levels that currently challenge conventional assay methods.

Appendix A

Multiplexing Assays

Fluorescence images of IL-18 and TNF multiplexing assays performed on a 20 μm striped ZnO nanorod platform. The ZnO nanorod platform was treated first with a mixture of primary IL-18 and TNF antibodies. After carrying out BSA blocking, a mixture of IL-18 and TNF with a predetermined concentration ratio was introduced to the assay platform. Then, a secondary, labeled IL-18 and TNF antibodies were reacted on the platform. Panels shown in A and B were obtained from the same ZnO nanorod platform area when the concentration ratio between IL-18 and TNF used in the assay was 20:1 and 2:1, respectively. Top and bottom panels show fluorescence from the IL-18 and TNF channels, respectively.

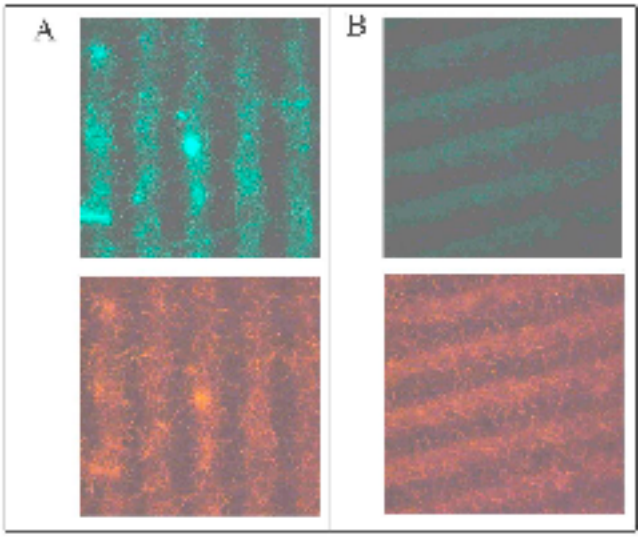

BIBLIOGRAPHY

Adalsteinsson, V., Parajuli, O., Kepics, S., Gupta, A., Reeves, B. & Hahm, J. 2008 Ultrasensitive Detection of Cytokines Enabled by Nanoscale ZnO Arrays. *Anal Chem* **80**, 6594-6601.

Brown, K., Fox, A. & Natan, M. 1996 Morphology-dependent electrochemistry of cytochrome c at Au colloid-modified SnO_2 electrodes. *J Amer Chem Soc* **118(5)**, 1154-1157.

Kim, H. & Juhyoun, K. 2005 Electrochemical determination of total alkaline phosphatase in human blood with a micropatterned ITO film. *J Electroanalytical Chem* **577(2)**, 243-248.

Konry, T., Heyman, Y., Cosnier, S., Gorgy, K. & Marks, R. 2008 Characterization of thin poly(pyrrole-benzophenone) film morphologies electropolymerized on indium tin oxide coated optic fibers for electrochemical and optical biosensing. *Electrochimica Acta* **53(16)**, 5128-5135.

Krishnamoorthy, S., Iliadis, A., Bei, T. & Chrousos, G. 2008 An interleukin-6 ZnO/SiO2/Si surface acoustic wave biosensor. *Biosensors & Bioelectronics* **24(2)**, 313-318.

Liu, G. & Lee, P. 2005 Optical sensing of electrochemical reactions on a bio-hybrid nanoparticle. *Proceedings of SPIE* **5705**, 123-130.

McKenzie, K., Marken, F. & Opallo, M. 2005 TiO_2 phytate films as hosts and conduits for cytochrome c electrochemistry. *Bioelectrochemistry* **66(1-2)**, 41-47.

Moore, E., O'Connell, D. & Galvin, P. 2006 Surface characterization of indium-tin oxide thin electrode films for use as a conducting substrate in DNA sensor development. *Thin Solid Films* **515(4)**, 2612-2617.

Ram, K., Bertoncello, P., Ding, H., Paddeu, S. & Nicolini, C. 2001 Cholesterol biosensors prepared by layer-by-layer technique. *Biosensors & Bioelectronics* **16(9-12)**, 849-856.

Salata, O. 2004 Applications of nanoparticles in biology and medicine. *J Nanobiotechnology* **2(3)**, 1-6.

Selvaraju, T., Das, J., Jo, K., Kwon, K., Huh, C., Kim, T. & Yang, H. 2008 Nanocatalyst-based assay using DNA-conjugated Au nanoparticles for electrochemical DNA detection. *Langmuir* **24(17)**, 9883-9888.

Tang, C., Kumar, S. & Chen, S. 2008 Zinc oxide/redox mediator composite films-based sensor for electrochemical detection of important biomolecules. *Anal Biochem* **380(2)**, 174-183.

Whicher, J. & Evans, S. 1990 Cytokines in disease. *Clinical Chem* **36**, 1269-1281.

Zang, J., Li, C., Cui, X., Wang, J., Sun, X., Dong, H. & Sun, C. 2007 Tailoring zinc oxide nanowires for high performance amperometric glucose sensor. *Electroanalysis* **19(9)**, 1008-1014.

Academic Vitae

Viktor Adalsteinsson

23 Fern Hill Road, Kennett Square, PA 19348
E-mail: viktor.adalsteinsson@gmail.com
Phone: (610) 742-7291

EDUCATION

Bachelor of Science, Chemical Engineering, 2010. Schreyer Honors College, Pennsylvania State University, **GPA: 3.96/4.00** *(3.98 in Chemical Engineering)*

Exchange Student in Chemical Engineering, University of Bath; Bath, UK. Spring 2008

TECHNICAL EXPERIENCE

Sanofi Pasteur. Bacterial (Vaccines) Technology. Swiftwater, PA. June – Aug. 2009.

- Developed a detoxification assay for a bacterial toxin based on physicochemical and immunochemical differences
- Validated CIP system for conjugated meningitis vaccine (Menactra) production
- Fermented *C. diphtheriae* at production scale for qualification lots within a DOE

Genentech, Inc. Process R&D: Early Stage Purification. Oceanside, CA. June – Aug. 2008.

- Evaluated a novel platform process for purifying monoclonal antibodies
- Conducted tech development DOE (Design of Experiment) on membrane adsorbers
- Attended all PR&D meetings, numerous technical seminars, and regularly presented experimental findings

Dr. Jong-in Hahm's Nano-Biotechnology Research Group, Pennsylvania State University, Department of Chemical Engineering. Dec. 2006 – *Present*.

- Conducting honors thesis research on the electrochemical detection of proteins using nano-electrodes
- Developing ultra-sensitive biosensors (femtogram mL^{-1} LLOD) for kidney disease markers such as Interleukin-18 and Tumor Necrosis Factor-Alpha
- Quantifying the fluorescence signal-enhancing effect of patterned nanomaterial substrates for protein/fluorophore-conjugated antibody interactions
- Evaluating diblock copolymer templates for protein adsorption phenomena

AviServe LLC. Delaware Biotechnology Park, Newark, DE. June – Aug. 2005.

- Conducted ELISA assays to detect antibody levels related to Infectious Bursal Disease Virus, Avian Leucosis Virus, and Hemmorhagic Enteritis Virus in various chicken blood and sera samples
- Inoculated chicken embryos to study the phenotypic effects of particular avian viruses
- Ran Agar Gel Precipitation to determine specific antibody/antigen interactions

PUBLICATIONS & CONFERENCES

1. **V. Adalsteinsson, O. Parajuli, S. Kepics, A. Gupta, W. Brian Reeves, J. Hahm**, Ultrasensitive Detection of Cytokines Enabled by Nanoscale ZnO Arrays, *J. Anal. Chem., 2008, 80 (17), pp 6594–6601*

2. **N. Kumar, O. Parajuli, A. Dorfman, V. Adalsteinsson, J. Hahm**, Engineering Nanorod Assay Platforms for Highly Sensitive and Specific Biomedical Detection, SBE's 4th International Conference on Bioengineering and Nanotechnology, July 2008, Presented by J. Hahm.

3. **American Chemical Society's National Meeting.** Philadelphia, PA. Aug. 2008. Attended technical seminars on downstream processing of monoclonal antibodies.

4. **Undergraduate Research at the Capital.** Harrisburg, PA. Oct. 2008. Represented Pennsylvania State University at undergraduate research poster session for state legislators. "Ultrasensitive Detection of Cytokines Enabled by Nanoscale ZnO Arrays."

INDEPENDENT STUDIES

Nonlinear Static and Dynamic Optimizations of Bioreactors with Intracellular Uptake Kinetics. Dr. Antonious Armaou, Department of Chemical Engineering, Pennsylvania State University. Spring 2009.

- Evaluated objective functions and constraints describing intracellular uptake kinetics
- Wrote and employed nonlinear optimization algorithms
- Obtained both optimal dilution rate and optimal dilution profiles for steady and unsteady state systems, respectively

Synthesis and Bioactivity of 4-Thiazolidinones. Dr. Jackie Bortiatynski and Dr. Sheryl Rummel, Department of Chemistry, Pennsylvania State University. Fall 2008.

- Conducted literature review of 4-thiazolidinone synthesis routes
- Synthesized both known and novel compounds for evaluation in bioassays

Nonlinear Dynamic Heat Transfer on a Catalytic Reaction Surface. Dr. Antonious Armaou, Department of Chemical Engineering, Pennsylvania State University. Fall 2008.

- Studied Hilbert Spaces and Galerkin Method

- Performed sensitivity analysis on unsteady state heat diffusion equation using finite elements in COMSOL Multiphysics

Cryogenic Separation of Methane and Hydrogen. Dr. Themistoklis Matsoukas, Department of Chemical Engineering, Pennsylvania State University. Fall 2007.

- Modeled process thermodynamics using AspenTech HYSYS software package
- Determined conditions to affect desired separation within thermodynamic constraints

HONORS & AWARDS

- National Science Foundation Graduate Research Fellow (GRFP)
- Schreyer Honors College Academic Excellence Scholarship
- Genentech PR&D "Outstanding Student Award" in Chemical Engineering
- William and Wyllis Leonhard Honors Program and Scholarship, College of Engineering
- David L. and Rena Miller Arm International Travel Program and Awards Endowment
- Undergraduate Research Fellowship in the Department of Chemical Engineering
- National Science Foundation REU Research Grant
- NFIB Young Entrepreneur Award
- Tau Beta Pi Honor Society
- Phi Kappa Phi Honor Society
- Dean's List

ACTIVITIES

American Institute of Chemical Engineers (AiChE), Omega Chi Epsilon (OXE) Chemical Engineering Honors Society, Tau Beta Pi Honor Society (TBP), International Society for Pharmaceutical Engineering (ISPE), International Programs Ambassador, Envisioneers (creativity-based engineering club for the Leonhard Honors Program), Intramural Soccer, College of Engineering Open House (presentations and tours), Chemical Engineering Prospective Student Days (department and laboratory tours)